ASTRONOMY & ASTROPHYSICS
SUPPLEMENT SERIES

JANUARY II **1998**, PAGE 327

Astron. Astrophys. Suppl. Ser. **127,** 327-333 (1998)

Crowded-field photometry from HST-imaging⋆

M. Sodemann and B. Thomsen

Institut for Fysik og Astronomi, Aarhus Universitet, Ny Munkegade, DK-8000 Århus C, Denmark

Received January 31; accepted May 9, 1997

Abstract. We present a thorough investigation of stellar photometry based on HST imaging of crowded fields at 85″ and 10″ from the centre of the high-surface brightness elliptical galaxy M 32. The Principal Investigators of the present archive data have elsewhere presented an impressive colour-magnitude diagram of the field at 85″. Based on the same data we enlarge on their photometric analysis and supplement with error estimators that more clearly show the implications of severe image crowding on the stellar photometry. We show that the faintest stars ($I \gtrsim 25.0$, $V \gtrsim 26.0$) are found too bright by several tens of a magnitude. For the field at 10″ we conclude that it is not possible to obtain reliable stellar photometry, standard deviations being larger than 0.4 mag. Artificial-star experiments show that only very few of the brightest stars of the luminosity function can be expected to represent single objects, the majority being either spurious or not as bright as measured. The paper as such introduces and demonstrates basic guide lines which may be used when dealing with stellar photometry of severely crowded fields.

Key words: methods: data analysis — galaxies: elliptical — galaxies: individual: M 32 — galaxies: stellar content

1. Introduction

In order to increase our knowledge of extra-galactic stellar systems like elliptical galaxies, we observe the average galaxy brightness, which gives rise to the traditional broad-band colours and spectral-line indices. In addition, we observe the variance of the galaxy brightness, i.e., the surface-brightness fluctuations (Tonry & Schneider 1988). Of course, the ultimative goal is to obtain stellar luminosity functions and colour-magnitude diagrams, i.e., accurate photometry of individual stars.

Until recently, colour-magnitude diagrams have been obtained solely from ground-based imaging of stars in our local neighbourhood, i.e., field stars and stars in open- and globular clusters of our Galaxy, in addition to approaches to Local Group dwarf spheroidals and the Magellanic Clouds (*low surface-brightness* stellar systems) from ground (e.g. Freedmann 1992) and space (e.g. Mighell & Rich 1996). Then Grillmair et al. (1996) presented an impressive colour-magnitude (CM) diagram of M 32, our closests elliptical and companion to the Andromeda galaxy, based on Hubble Space Telescope imaging (archive data, ID 5233). Using the same data we have been able to reproduce the CM diagram of M 32 which in itself, however, was not the main goal of our work. We have carried out an investigation of the reliability of the CM diagram, that is, an estimation of the photometric quality of the detected stars. The image crowding in dense fields like that of the *high surface-brightness* elliptical M 32 may cause spurious detections and severely reduce the reliability of the photometry. In the present paper we discuss specific aspects of the photometric quality of extra-galactic stellar systems, aspects that supplement the discussion by Grillmair et al.

In our latest paper (Sodemann & Thomsen 1996) we presented ground-based imaging of M 32 obtained with the Nordic Optical Telescope with a seeing of FWHM $\sim 1\farcs0$ using $0\farcs175$ pixels. We identified a systematic variation in the I and B-band Surface-Brightness Fluctuations (SBF) of $0.2-0.3$ mag in the radial range $10'' \lesssim R \lesssim 50''$. In our search for the stars responsible for this variation we made a comparison of simulated stellar fields with the ground-based SBF observations. From this it became clear that it was not possible to supplement the measurements of the SBF with stellar photometry of the most luminous stars, due to excessive crowding.

However, at least in some cases the superb resolution of the Hubble Space Telescope's (HST) Wide Field Planetary Camera 2 – the Planetary Camera (PC) with seeing of FWHM $0\farcs1$ using $0\farcs05$ pixels – makes it possible to resolve

Send offprint requests to: bt@obs.aau.dk

⋆ Based on observations made with the NASA/ESA Hubble Space Telescope, obtained from the data archive at the Space Telescope Science Institute. STScI is operated by the Association of Universities for Research in Astronomy, Inc. under the NASA contract NAS 5-26555.

more than just the very brightest stars. Grillmair et al. (1996) presented a CM diagram based on HST-imaging of a region 85″ from the centre of M 32. From the surface brightness μ of M 32 we can compare this off-centre field with a central field at 10″ from the centre. Assuming that the same type of stars are responsible for the surface brightness at the two distances, the number of stars per area is ~ 40 times higher in the central field ($\mu^I_{85''} \simeq 19.8$ and $\mu^I_{10''} \simeq 15.8$). This merely indicates differing problems introduced by image crowding, problems that may turn up when dealing with CM diagrams of fields at various distances from the galaxy centre. We shall return to this later.

When discussing luminosity functions and CM diagrams we are interested in knowing to what magnitude limit we have actually been able to observe stars, a limit set mainly by a compromise between the image crowding and resolution, and the amount of exposure time. This magnitude limit is usually measured by addition and retrieval of a small number of faint artificial stars, that is, the test of (in)completeness. However, whereas the traditional method of adding artificial stars estimates the detection probability it does not measure the photometric quality of the detected stars or the effects of spurious detections caused by severe image crowding. That is, the estimate of the limiting magnitude is based on information about the location (the coordinates) of the added/recovered star alone and not on the magnitude of the recovered star. For the data presented here, one important result of the image crowding is the following: An artificial star of known magnitude added to the programme frame may be recovered with a magnitude up to $1^{\rm m}$ brighter than its original magnitude, but it turns out that it is not equally likely that this star will be recovered with a magnitude $1^{\rm m}$ fainter than its original magnitude. (In Sect. 3 we show that the asymmetry in the distribution of recovered stars cannot be explained as a result of plotting the data as a function of magnitude). Thus, the typical measure σ, the standard deviation, of the accidental error at a given magnitude is not an adequate description for this asymmetric distribution of recovered stars and has to be supplemented with additional error estimates.

Drukier et al. (1988) raised the problem of "bin jumping" and pointed out a way to account for this when correcting a measured luminosity function for incompleteness. LePoy et al. (1993) also discuss the effects of severe image crowding, which may produce an artificial enhancement of the bright end of the measured luminosity function if not dealt with in an appropriate way (see also Renzini 1992; Martinez-Delgado & Aparicio 1997).

We shall concentrate on the implications of crowding on stellar photometry of HST imaging of extra-galactic systems like the compact elliptical galaxy M 32. We begin with a description of the data and image handling (Sect. 2). After that follows a discussion on the artificial-star experiments in connection with the off-centre field at 85″ from the centre of M 32 (Sect. 3) and the dense central field at 10″ (Sect. 4). We summarise the results in Sect. 5.

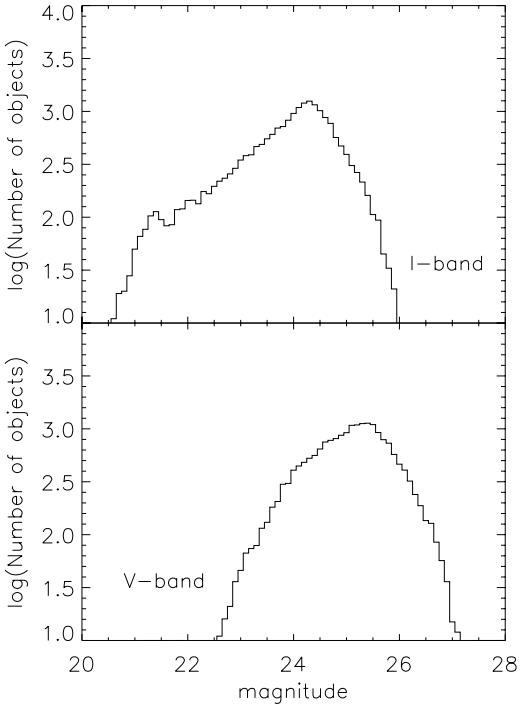

Fig. 1. Luminosity functions for objects identified in I and V, respectively, in the HST PC-frame at 85″ from the centre of M 32. A total of 19461 stars were found to match in I and V. No correction for M 31 has been made, see text. The slope of the I-band luminosity function is found to be 0.42. (This value is not used elsewhere in this paper)

2. Data and image handling

The observational basis for this paper is HST imaging of an off-centre field at 85″ from the centre of M 32 taken with the WFPC2 on October 22, 1994 (standard-calibration observations, archive data, ID 5233). See Grillmair et al. Figs. 1 and 2 for an outline of the M 32 PC field on the sky. The 2×4 500 s frames in F555W (V) and F814W (I), respectively, were co-added through the cosmic-ray removing software of Groth & Shaya (1992) resulting in two programme frames. An I-band programme frame of the field at 10″ was produced in a similar way from 3 exposures of 400 s each (archive data, ID 5464). Correction for vignetting was carried out according to Holtzman et al. (1995a), and standard magnitudes and colour were derived using the calibrations in Holtzman et al. (1995b). We have adopted $A_I = 0.14$ for the galactic absorption (Burstein & Heiles 1984; Cardelli et al. 1989): The luminosity functions and CM diagrams have been corrected for this.

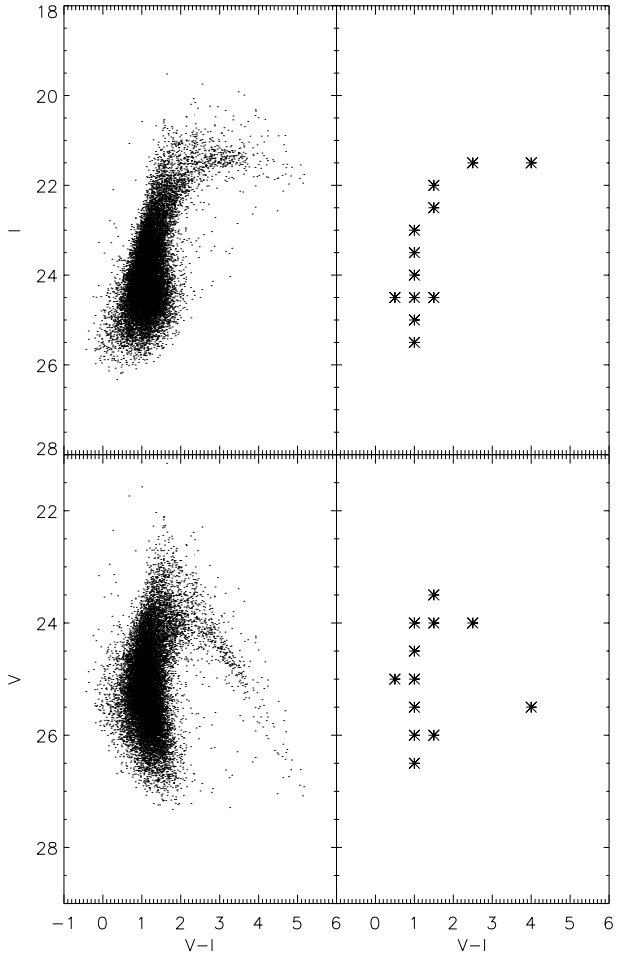

Fig. 2. Colour-magnitude diagram of the off-centre field in M 32. This figure was produced by matching the objects in Fig. 1. The 2×12 star signs show the magnitude and colour of the stars in our artificial-star experiments

The programme frames did not contain sufficiently bright, isolated stars to define a proper point-spread function (PSF). Therefore, model PSFs generated by the program Tiny Tim (Krist 1993) defined the artificial stars added during the completeness tests and the master PSF of the psf-fitting software by Stetson's (1987) DAOPHOT II package.

The completeness tests were carried out by adding stars distributed according to the observed CM diagram. The 2×12 star signs in Fig. 2 for I and V, respectively, outline the range of magnitudes and colours. A total of 7110 artificial stars were added to each of the two programme frames. When carrying out an addition of stars, only very few (in principle *one*, or several laid in a grid) ought to be added at a time so as to avoid confusion between added stars and an increase of the image crowding. As an alternative, we split the addition of the artificial stars into two and those stars which happened to be added near another artificial star were removed. The stars were added using our HST-Sim routines, which scale and add the required number of PSFs (the routines are implemented using Interactive Data Language, IDL). The routines take into account the geometric distortion inherent in the WFPC2 optical system, and shifting and rebinning of the subsampled PSFs provide subpixel positioning. Finally, Poissonian photon noise and Gaussian read noise are added.

The photometry of objects in the programme frames was obtained through a procedure that included several passes of object identification and measurement of magnitudes, using DAOPHOT II. First we worked through the identification of objects in the I-frame. In order to identify as many objects as possible and to ease the identification of faint objects we carried out ~ 6 iterations, successively reaching fainter magnitudes. For every two iterations we concatenated the lists of hitherto revealed stars, subtracted those from the original frame, and continued from there. The iterations ended when we reached a threshold of 4 standard deviations of the background level, as calculated by DAOPHOT - at that point only a few hundred stars were identified and successfully subtracted by ALLSTAR and an additional iteration did not provide more objects. The final ALLSTAR list of all stars in I was then applied for star-subtraction in the V frame. After having calculated flux-averaged positions based on the I and V list of objects we again ran ALLSTAR on both frames, now with fixed coordinates. In this way a total of 19461 stars were found to match in V and I. The photometry of the star-added frames was carried out in a way identical to that of the programme frames.

Note, Grillmair et al. applied Stetsons's (1994) photometry package ALLFRAME. They found that the global characteristics of the CM diagram produced using DAOPHOT II/ALLSTAR were essentially identical to those found using ALLFRAME.

We have made no attempts to correct for the M 31 background stars as none of the conclusions of this paper depend on knowing this accurately. According to Grillmair et al. about 18% of the $\sim$ 20000 stars identified in the programme frames originate in M 31.

3. Results from the off-centre field

The luminosity functions and CM diagrams of the off-centre field of M 32 are seen in Figs. 1 and 2. With the artificial-star experiments as our basis we will now discuss the uncertainty associated with the identified stars.

In Figs. 3 and 4 the magnitude of each group of added stars is indicated by a vertical line. The magnitudes of the recovered stars are binned into histograms of $0\overset{\mathrm{m}}{.}1$ bins, one histogram for each magnitude group of added stars. Each of the histograms has been normalised so that they all cover the same number of stars (implying that the number-axis is arbitrary). This illustrates that the

brightest stars are easily identified, whereas fainter stars are "spread out" from their original magnitude (the vertical line) to surrounding magnitudes. Firstly, note that for the faintest bins the probability of a star being found in a bin other than the one to which it was added is nonvanishing. If we want to correct the luminosity function for incompleteness, this "bin jumping" has to be taken into account (Drukier et al. 1988). Secondly, the "bin jumping" is clearly asymmetric with an extended tail of bright measurements. As the measurement errors are clearly not Gaussian we shall replace the usual, but now inadequate, standard deviation σ by the mean absolute deviation (MAD). (The MAD is related to the median as the standard deviation is related to the mean, but the MAD does not require that the distribution of the errors is Gaussian and it is a more robust estimator than is the mean, Press et al. 1992). In addition, we supplement with the lower and upper quartile, and several percentiles, of the magnitude of the recovered star $m_{\rm rec}$. These numbers are indicated in Figs. 3 and 4 and illustrate that the faintest stars in the CM diagram are very likely identified too bright by several tens of a magnitude as compared to their true, unaffected magnitude.

Note, the straight lines represented by diamond symbols in Figs. 3, 4, and 9 indicate the magnitude of the added stars $m_{\rm add}$ and the expected magnitude of the recovered stars *if they are not affected* by "binjumping", i.e., $m_{\rm rec} = m_{\rm add}$. In order to claim that we are able to carry out reliable photometry, $m_{\rm add}$ must be a unique function of $m_{\rm rec}$, and we must be certain that we are measuring the added star and not a statistical lump of unresolved stars.

The distribution of the colour of recovered stars is, however, fairly symmetric and much less wide than that of the two passbands individually (Fig. 5). That is, the added stars which undergo "bin jumping" tend to keep their original colour, mainly because they are most likely identified on top of a star with a colour similar to their own – the majority of stars in the CM diagram are found along the giant branch with $(V - I) \simeq 1.0$. We may therefore expect that the colours of the stars in the CM diagram are correct.

Figure 6 illustrates that the asymmetric distribution in the histogram of recovered stars is not a result of plotting the number of stars as a function of magnitude. We generated a Gaussian distribution of fluxes according to $\mathrm{d}N = N_0 \mathrm{e}^{-(f-f_0)^2/2\sigma^2}\mathrm{d}f$, where $N_0 = 10^6$, $f_0 = 1.0$, and $\sigma = 0.4$. The corresponding magnitudes $m = -2.5 \log f$ were binned into $0\overset{\rm m}{.}1$ bins. The increase in the number of stars fainter than f_0 ($m > 0$) exceeds a small increase just below $m = 0$ and is clearly opposite the asymmetry seen in Figs. 3 and 4. Note that Secker & Harris (1993) adopt a Gaussian function to represent the measurement error as a function of magnitude.

The limiting magnitudes at half probability are $V_{1/2} = 26.2$ and $I_{1/2} = 25.1$ for the M 32 off-centre field. The limiting magnitudes are based on *all* the stars plotted in Figs. 3 and 4, respectively, i.e., regardless of the associated error estimate. Note, the standard deviation σ, as calculated by ALLSTAR, amounts to only $0\overset{\rm m}{.}12$ and $0\overset{\rm m}{.}16$ at the limiting magnitudes for I and V, respectively, whereas the MAD is higher by a factor of 3.8 and 2.8 as compared to the standard deviation (for a Gaussian distribution MAD $\simeq 0.8\sigma$). This merely indicates that in the present investigation the standard deviation, as given by ALLSTAR, may be considered too optimistic.

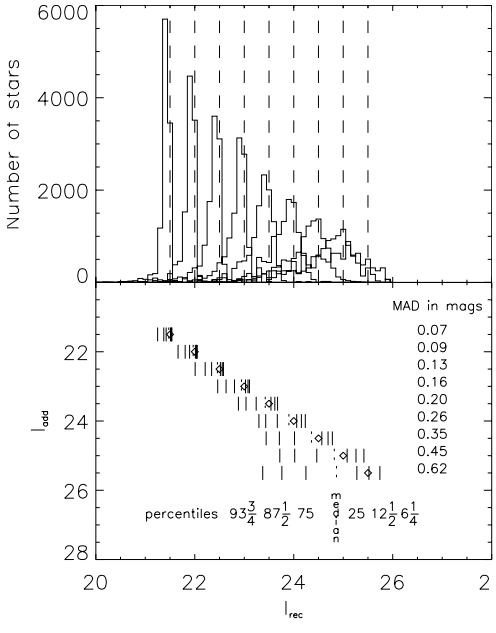

Fig. 3. Results of our I-band artificial-star experiments. For each magnitude group of added stars (vertical line) the histogram of recovered stars is shown. Note, the number-axis is arbitrary (Sect. 3). To clarify the implications of image crowding we plot several error indicators, in addition to the mean absolute deviation (MAD), of the magnitude of the recovered star $m_{\rm rec}$. This demonstrates that the distribution of recovered stars is skewed towards brighter magnitudes, that is, the faintest objects are found too bright. This "bin jumping" was discussed by Drukier et al. (1988)

4. The M 32 centre

Based on the investigation of the off-centre field it is possible to predict the number of identified stars in a central field at about $10''$, where the density is ~ 40 times higher than in the off-centre field (Sect. 1). The I-band luminosity function of the off-centre field starts to turn over at a number density of $\sim$ 1000 per $0\overset{\rm m}{.}1$ in the PC frame (Fig. 2). In a field with density 40 times higher than this, the turn-over would correspond to a magnitude of $\sim 20\overset{\rm m}{.}5$, or at the very brightest end of the luminosity function where the number density drops to zero. An interesting question is whether it is possible to find stars of $20\overset{\rm m}{.}4$ in the central region of M 32. (This magnitude corresponds

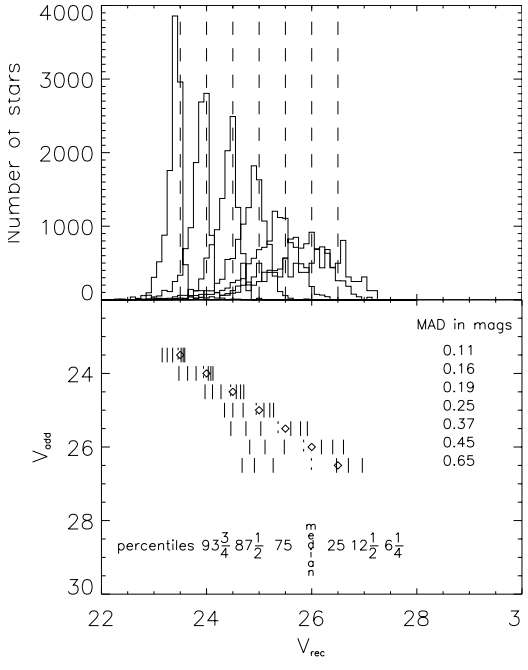

Fig. 4. Same as Fig. 3 but now for the V-band

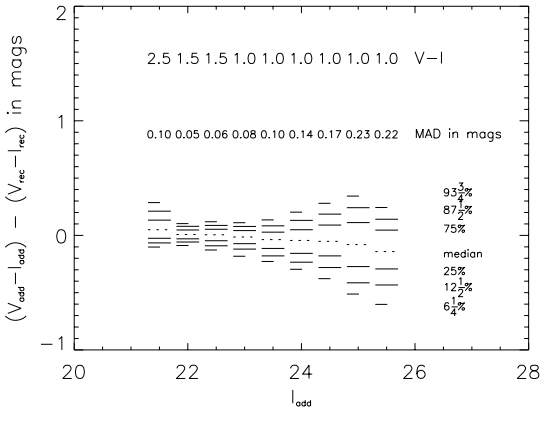

Fig. 5. Colour deviation of recovered stars for the 9 artificial I-band magnitudes (error indicators are as in Figs. 3 and 4). This shows that stars are very likely to be found with the correct colour. The explanation is that the majority of stars in the CM diagram (Fig. 2) have more or less identical colours $(V-I) \simeq 1.0$

to $M_I \simeq -4.0$, the expected tip of the red-giant branch for metal-poor stars, e.g. Lee et al. 1993, and could provide an estimate of the distance to the galaxy). To address this question we have investigated a central field in M 32 (archive data, ID 5464), the analysis being virtually identical to that of the off-centre field. (The addition of artificial stars was split up so that no more than one magnitude group at a time, corresponding to ~ 700 stars, was added to the programme frame). The luminosity function of the central field is seen in Fig. 7.

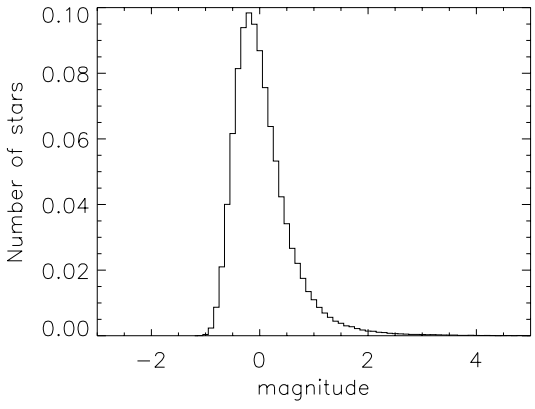

Fig. 6. Asymmetry that arises due to the effect of plotting a histogram of stars as a function of magnitude $m = -2.5 \log f$, where the distribution in flux f is Gaussian (arbitrary number-axis). The asymmetry is opposite that of the histograms in Figs. 3 and 4

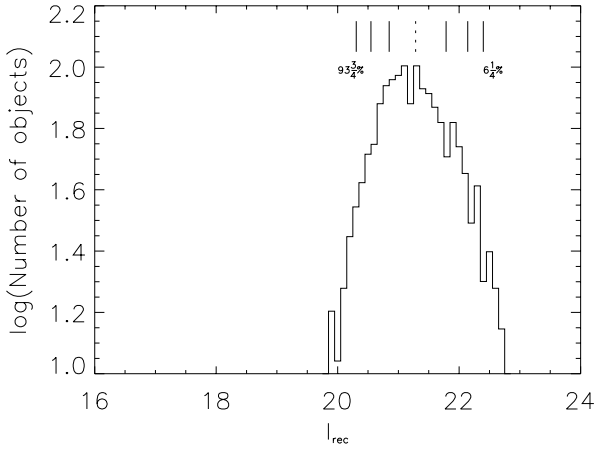

Fig. 7. Luminosity function for objects identified in I in the HST PC-frame centered on M 32. A total of 1606 objects were found in an annulus of area $80''^2$ and radius $\sim 10''$. The median indicated at the top is $21\overset{\mathrm{m}}{.}3$. Only a few of the very brightest stars can be considered to be single objects

Apparently we do see stars of magnitude $20\overset{\mathrm{m}}{.}4$ (Fig. 7). However, when we discuss the central field, we also have to consider the confusion that spurious detections due to SBF may cause, i.e., the confusion between single objects and detection of statistical lumps in the background of unresolved stars (they both have the shape of the PSF). This problem is illustrated in Fig. 8 where we see that bright objects around, e.g., $20\overset{\mathrm{m}}{.}4$ are indeed detected and located in the recovery tests with artificial stars of magnitude $21\overset{\mathrm{m}}{.}0$ and fainter. The completeness tests show that *if* stars of magnitude $20\overset{\mathrm{m}}{.}4$ are present in the centre of M 32, then we will be able to identify them (the data in Fig. 8 imply a limiting magnitude at half probability of $I_{1/2} = 21.6$ for the central field of M 32). What we do not know is how large a fraction of the supposedly identified

bright stars in Fig. 7 are merely compounds of fainter, unresolved stars. The limiting magnitude itself gives us no information about that.

As will be evident from the following, we can only expect very few of the brightest stars of the observed luminosity function to be single objects. Figure 9 illustrates that it is not possible to distinguish between the distributions of stars added at $\sim 20\overset{\mathrm{m}}{.}5$ and fainter. That is, when we identify a star with magnitude $\sim 20\overset{\mathrm{m}}{.}5$ or fainter, then we can by no means tell the true magnitude of that star. The completeness tests imply a limiting magnitude of $I_{1/2} = 21.6$ as mentioned above, but this limit only indicates the detection probability. We are inclined to disregard the stars in Fig. 7 that are fainter than $\sim 20\overset{\mathrm{m}}{.}5$ (i.e., even stars brighter than $I_{1/2}$), since we have no reason to believe that they are single point sources.

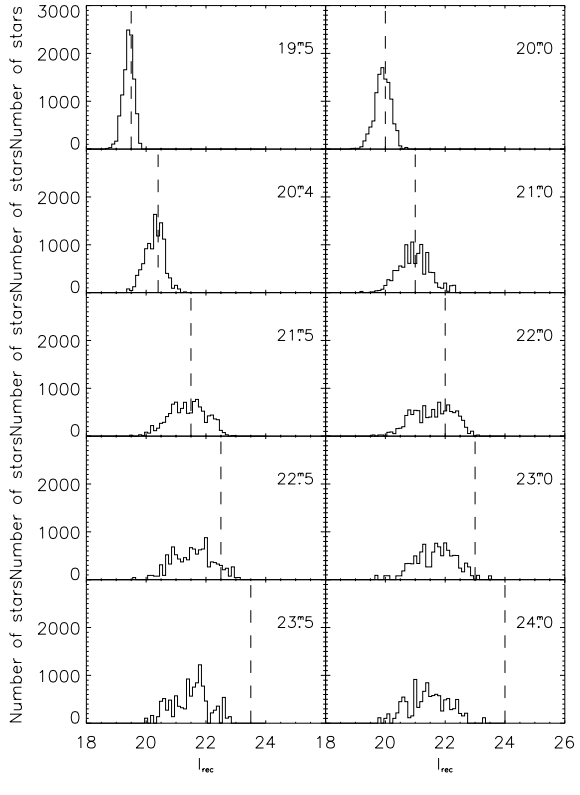

Fig. 8. Results of our I-band artificial-star experiments, now for the central region of M 32, approximately $10''$ from the centre. Again, the number-axis is arbitrary (Sect. 3)

This is further emphasised by a simple simulation of the stellar field at $10''$: As the stellar content we adopt only one type of stars, namely stars of magnitude $\bar{m}_I = 22.78$ (Sodemann & Thomsen 1996). Our HST-Sim routines add the required number of such "fluctuation stars" (PSFs) of magnitude $\bar{m}_I$ to reach the average surface brightness of $\mu^I_{10''} \simeq 15.8$ as observed for the central frame, and photometry is carried out by DAOPHOT II. The luminosity function of this simulated stellar field is seen in Fig. 10 and should be compared with the luminosity function of the observed central field (Fig. 7). The similarities are striking and tell us that the objects in Fig. 7 may all, except for a very few of the brightest, be described as mere fluctuations and not as single point sources. Based on Fig. 10 we may explain the observed "skewness" in Fig. 9 as follows. Those of the faint added stars which were located on top of a bright fluctuation have inevitably been measured too bright and therefore end up in the left part of the "magnitude bands" of recovered stars (a magnitude band being defined by the 93.75 and 6.25 percentiles), whereas the stars in the right part of the "magnitude bands" were located on top of a less bright fluctuation.

We do not correct the observed luminosity functions for incompleteness and binjumping for the following reasons. Concentrating on the I-band, for the field at $85''$ the histograms of recovered stars are distinguishable for magnitudes that correspond to the giant branch and down to $I \simeq 24.0$ where incompleteness starts to set in (Figs. 1 and 3). In this paper we do not require the incompleteness-corrected luminosity function, and correction for binjumping would only affect the magnitudes around the limiting magnitude. For the field at $10''$, the luminosity function is comparable to any of the distributions of added test stars fainter than $\sim 20\overset{\mathrm{m}}{.}5$, and an attempt to deconvolve the effects of "binjumping" would thus be an ill-posed problem.

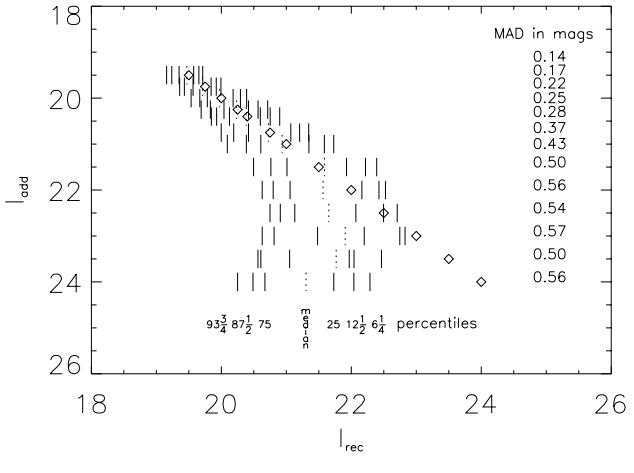

Fig. 9. Same data as Fig. 8 (besides three extra sets of artificial stars) but plotted in a slightly different way (error indicators are as in Figs. 3 and 4). As emphasized in the text, m_{add} must be a unique function of m_{rec}, and we must be certain that we are measuring the added star and not a statistical lump of unresolved stars, before we can claim that we are able to carry out reliable photometry. This is clearly not the case for magnitudes fainter than $\sim 20\overset{\mathrm{m}}{.}5$. From that magnitude and onwards it is no longer possible to distinguish between the distributions of recovered stars. Therefore, only a few of the very brightest stars with $I \lesssim 20.5$ in Fig. 7 may be expected to be single objects

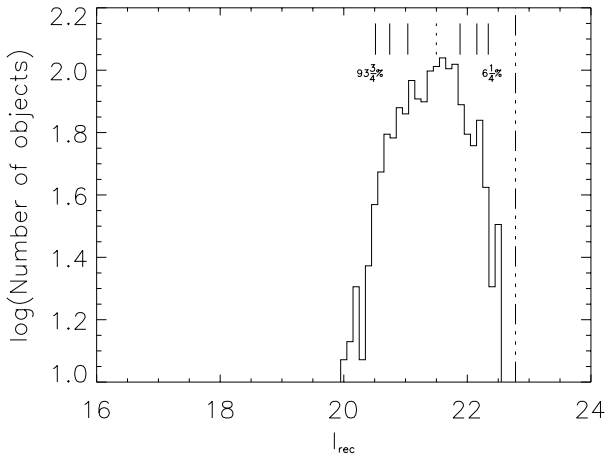

Fig. 10. Luminosity function of a simulated stellar field with $\mu^I_{10''} \simeq 15.8$, as observed for the central field, but generated from only *one* type of stars, namely stars of magnitude $\bar{m}_I = 22.78$ (vertical line), see text. Note the similarities to the observed luminosity function (Fig. 7). The median indicated at the top is $21\overset{\text{m}}{.}5$. (The histogram above has been normalised to the same number of objects as that of Fig. 7)

5. Conclusion

In this paper we have discussed the effects that severe image crowding has on stellar photometry. The investigation covered two fields of the high-surface brightness elliptical galaxy M 32 observed with the HST's PC (archive data, ID 5233 and 5464).

We have carried out a large number of artificial-star experiments, that is, addition and retrieval of artificial stars. Our experiments clearly show the presence of "binjumping": The faint stars added to the programme frames are recovered too bright; the fainter the star and the denser the field, the bigger is the effect of "binjumping". The traditional indicator of (in)completeness of the photometry, $m_{1/2}$, merely provides a detection probability but not the quality of the photometry.

For the less dense field at 85″ from the centre of M 32, the effects of image crowding show up around the limiting magnitude $I_{1/2}$ ($25\overset{\text{m}}{.}1$). Stars fainter than that are found too bright by several tens of a magnitude as compared to their true magnitude, whereas their colour is mainly unaffected. For the far more dense field at 10″ from the centre, "binjumping" affects stars that are even brighter than $I_{1/2}$ ($21\overset{\text{m}}{.}6$). As our Fig. 9 demonstrates, only the very brightest stars with $I \lesssim 20\overset{\text{m}}{.}5$ may be considered to represent single objects. Thus, we do measure single stars of, e.g., $20\overset{\text{m}}{.}4$ (corresponding to $M_I \simeq -4.0$, the expected tip of the red-giant branch for metal-poor stars) in the off-centre field at 85″, but based on the present data it is not possible to claim that for the central field at 10″, where the density is 40 times higher.

Finally, we would like to emphasize that the data analysis, which has been introduced and described in the present paper in relation to HST imaging, should be carried out for essentially all imaging of severely crowded fields.

Acknowledgements. We wish to thank P.B. Stetson for the benefits of using his photometry package DAOPHOT II.

References

Burstein D., Heiles C., 1984, ApJS 54, 33
Cardelli J.A., Clayton G.C., Mathis J.S., 1989, ApJ 345, 245
Drukier G.A., Fahlman G.G., Richer H.B., 1988, AJ 95, 1415
Freedman W.L., 1992, in The Stellar Population of Galaxies, Barbuy B., Renzini A. (eds.) Proc. IAU Symp. 149. Dordrecht: Kluwer, p. 169
Grillmair C.J., Lauer T.R., Worthey G., et al., 1996, AJ 112, 1975
Groth E., Shaya E., 1992, in Final Orbital/Science Verification Report, Faber S.M., Westphal J.A. (eds.) STScI, Baltimore, Chap. 14
Holtzman J.A., Hester J.J., Casertano S., et al., 1995a, PASP 107, 156
Holtzman J.A., Burrows C.J., Casertano S., et al., 1995b, PASP 107, 1065
Krist J., 1993, in Astronomical Data Analysis Software and Systems II, ASP Conf. Ser. 52, Hanisch R.J., Brissenden R.J.V., Barnes J. (eds.), p. 530
Lee M.G., Freedman W.L., Madore B.F., 1993, ApJ 417, 553
LePoy D.L., Terndrup D.M., Frogel J.A., et al., 1993, AJ 105, 2121
Martinez-Delgado D., Aparicio A., 1997, ApJ 480, L107
Mighell J.M., Rich R.M., 1996, AJ 111, 777
Press W.H., Flannery B.P., Teukolsky S.A., Vetterling W.T., 1992, in Numerical Recipes in C. – 2nd ed. Cambridge University Press, p. 611
Renzini A., 1992, in Galactic Bulges, DeJonghe H., Habing H. (eds.) Proc. IAU Symp. 153. Dordrecht: Kluwer, p. 151
Secker J., Harris W.E., 1993, AJ 105, 1358
Sodemann M., Thomsen B., 1996, AJ 111, 208
Stetson P.B., 1987, PASP 99, 191
Stetson P.B., 1994, PASP 106, 250
Tonry J.L., Schneider D.P., 1988, AJ 96, 807